NUMERICAL SIMULATION OF DROPLET DISPERSION AND EVAPORATION WITH A MOMENTS-BASED CFD MODEL

João N. E. Carneiro, carneiro@td.mw.tum.de
Volker Kaufmann, kaufmann@td.mw.tum.de
Wolfgang Polifke, polifke@td.mw.tum.de
Lehrstuhl für Thermodynamik, Faculty of Mechanical Engineering, Technische Universität München, Boltzmannstraße 15, 85748 Garching, Germany

Abstract. *In the present work, a CFD model to simulate droplet dispersion and evaporation is presented. In order to take into account the inherent polydispersity of this type of flow in an efficient way, Eulerian transport equations are solved for the moments of the size distribution function and the disperse phase volume average velocity in addition to the common conservation equations for a turbulent gas phase. Closure for mass, momentum and heat exchange terms is achieved with help of a presumed Number Density Function for the droplet size spectrum. The model is implementend in the open source code OpenFOAM extending a previously developed isothermal, incompressible Two-Fluid solver. The model is tested for a spray generated by an ultra-sonic atomizer and simulation results are compared against experimental data of Baessler, Moesl and Sattelmayer (2007) showing good agreement for both isothermal and evaporating cases.*

Keywords: *Spray; Polydisperse; Moments Model; Presumed Number Density Function*

1. INTRODUCTION

The numerical simulation of droplet flows is still considered a challenging task and an open field for research. Eulerian-Eulerian models represent an interesting alternative to Lagrangian techniques since they are computationally less expensive and are also able to capture the most important characteristics of the flow. In Multi-Fluid models, each particle size group is treated as a different Eulerian phase, hence polydispersity can in theory also be automatically captured. However, solving sets of transport equations for each class (or groups of classes) for the whole computational domain restricts the approach to a limited number of size classes, and Lagrangian models are generally recognized to be more efficient in this regard (see Mostafa and Mongia, 1987). Recently, alternative approaches have been developed, which make possible to account for effects of polydispersity with reduced computational effort. These methods rely upon formulations involving moments (or some other information) of the particle size distribution function to determine the disperse phase dynamics and its interaction with the continuous phase flow. Examples can be found in the work of Beck and Watkins (2003) and Fox, Laurent and Massot (2008).

In the present work, a novel moments approach is presented which consists of the integration over the size spectrum of the droplet equations written in an Eulerian frame, resulting in transport equations for the moments and its transport velocities. Extra modeling effort is required for closure of the interphase exchange terms depending on unknown moments, which is achieved with help of a presumed Number Density Function (pNDF) of the Gamma type. This assumption allows an easy reconstruction of the distribution from low order moments and the calculation of quantities required to represent the effect of the droplets on the continuous phase (and vice-versa). However, care must be taken in the reconstruction process, as the outcome of the solution process might generate invalid moment sets; i.e., an unphysical combination of moments which has no corresponding distribution function. As suggested by Wright (2007), positiveness of Hankel-Hadamard determinants must be achieved throughout the flow field in order to guarantee conditions necessary for the reconstruction of a distribution function to a given set of moments. This will be shown to be the case here for an evaporating spray, where different source terms for the moments are considered.

The next section is dedicated to the derivation of the model equations, followed by a brief description of the numerical implementation in OpenFOAM. Finally, results for non-evaporative and evaporative test cases are presented and compared to the data of Baessler, Moesl and Sattelmayer (2007), followed by conclusions and outline of future research.

2. MATHEMATICAL MODEL

The moments of the size distribution function $f(D)$ are defined as:

$$M^{(k)} \equiv \int_0^\infty D^k f(D) dD. \tag{1}$$

A physical interpretation for each of the moments follows:

- $M^{(0)}$: total number of particles (per unit cell-volume)

- $M^{(1)}$: sum of the particle diameter ($\shortparallel$)
- $\pi M^{(2)}$: total surface area of particles ($\shortparallel$)
- $\frac{\pi}{6} M^{(3)}$: total volume of particles ($\shortparallel$); or the local volume fraction of the disperse phase

The moment transport velocities are defined for the k^{th} moment as:

$$\mathbf{u}^{(k)} \equiv \frac{1}{M^{(k)}} \int_0^\infty \mathbf{u}(D) D^k f(D) dD, \tag{2}$$

which are related to the integral over size and velocity spectra; $f(D)$ and $\mathbf{u}(D)$, respectively. Hence, $u^{(k)}$'s are the mean velocities at which the moments are convected[1]. They will only be the same (and equal to the dispersed phase velocity) in two limiting cases: for a monodisperse distribution; or if all particles have the same velocity. Otherwise, there is no reason, e.g., for $\mathbf{u}^{(2)}$ and $\mathbf{u}^{(3)}$ to be the same, as they are surface area and volume average velocities, respectively.

As will be shown next, the moments and its transport velocities appear automatically in the derivation of the model as a result of the integration of the Eulerian droplet equations over the diameter spectrum. The resulting set of equations are solved in addition to the conservation equations for a turbulent gas phase. The idea is to minimize computational costs while being able to capture the polydispersity of the flow through the correct description of the evolution of the moments.

2.1 Disperse Phase Equations

The mass conservation for a disperse phase can be written in the Eulerian framework as:

$$\frac{\partial \alpha \rho_d}{\partial t} + \boldsymbol{\nabla} \cdot (\alpha \rho_d \, \mathbf{u}) = \Gamma_d, \tag{3}$$

with ρ_d the density of the disperse phase and Γ_d the mass exchange rate (per unit volume) due to evaporation. In the present context, α should be interpreted as the local volumetric fraction of droplets belonging to the same size class.

The droplet momentum equations are derived by Crowe, Sommerfeld and Tsuji (1998):

$$\frac{\partial \alpha \rho_d \, \mathbf{u}}{\partial t} + \boldsymbol{\nabla} \cdot (\alpha \rho_d \, \mathbf{u} \, \mathbf{u}) = \mathbf{M} + \boldsymbol{\nabla} \cdot (\alpha \, \boldsymbol{\tau_d^t}) + \Gamma_d \, \hat{\mathbf{u}}_i. \tag{4}$$

The term $\Gamma_d \, \hat{\mathbf{u}}_i$ represents the momentum exchange due to evaporation and $\hat{\mathbf{u}}_i$ is taken to be equal to the droplet velocity. τ_d^t – the so called "disperse phase Reynolds stress term" – is usually modeled with the Boussinesq approximation

$$\boldsymbol{\tau_d^t} = \rho_d \, \nu_d^t (\boldsymbol{\nabla} \mathbf{u} + \boldsymbol{\nabla} \mathbf{u}^T - \frac{2}{3} \boldsymbol{\nabla} \cdot \mathbf{u} \, \mathbf{I}) - \rho_d \frac{2}{3} k_d \mathbf{I}, \tag{5}$$

where the disperse phase turbulent viscosity ν_d^t and turbulent kinetic energy k_d were introduced. Models for these terms will be presented later in conjunction with the turbulence model for the gas phase.

The momentum interaction term $\mathbf{M}$ appearing above is a mere transposition to the average flow of the local instantaneous form of hydrodynamic forces acting on each droplet. This will include, in the present work, the mean pressure gradient, shear stress, drag and turbulent dispersion forces. Other effects such as lift or virtual-mass will be neglected, as usually done in applications involving droplet flows. Hence:

$$\mathbf{M} = -\alpha \boldsymbol{\nabla} p + \alpha \boldsymbol{\nabla} \cdot \boldsymbol{\tau_c} + \mathbf{M}_{Drag} + \mathbf{M}_{TD}. \tag{6}$$

$\mathbf{M}_{Drag}$ is determined by:

$$\mathbf{M}_{Drag} = \frac{3}{4} \frac{C_D}{D} \alpha \rho_c |\mathbf{u}_r| \mathbf{u}_r, \tag{7}$$

with ρ_c the continuous phase density and the drag coefficient C_D being given by the Schiller-Naumann correlation:

$$C_D = \frac{24}{\mathrm{Re}} (1 + 0.15 \, \mathrm{Re}^{0.687}). \tag{8}$$

[1] Implicit here is the assumption that particles with the same size have locally the same velocity

The droplet Reynolds number (Re) can be written as: $\mathrm{Re} = \frac{|\mathbf{u}_r|D}{\nu_c}$; ν_c is the kinematic viscosity of the continuous phase.

$\mathbf{M}_{TD}$ is given according to Oliveira and Issa (1998) by:

$$\mathbf{M}_{TD} = \frac{3}{4}\frac{C_D}{D}\rho_c|\mathbf{u}_r|\frac{\nu_c^t}{\sigma_\alpha}\boldsymbol{\nabla}\alpha, \tag{9}$$

with $\sigma_\alpha = 0.7$.

The same idea can be applied for the energy equation of a single droplet, yielding an Eulerian equation for the specific internal energy i of a dispersed phase:

$$\frac{\partial \alpha\rho_d i}{\partial t} + \boldsymbol{\nabla}\cdot(\alpha\rho_d\,\mathbf{u}\,i - \alpha\rho_d\frac{\nu_d^t}{\mathrm{Pr}_d^t}\boldsymbol{\nabla}T) = Q_d + \Gamma_d\hat{h}_i, \tag{10}$$

with the heat flux at the interface being given by $Q_d = \frac{6\alpha}{D^2}\mathrm{Nu}\lambda_c(T_c - T)$ and $\hat{h}_i$ the sum of internal energy and latent heat of evaporation; $\hat{h}_i = i + \Delta h_v$. The Nusselt number (Nu) can be in turn determined with the correlation due to Ranz-Marschall: $\mathrm{Nu} = 2 + 0.6\mathrm{Re}^{\frac{1}{2}}\mathrm{Pr}^{\frac{1}{3}}$.

2.2 Moments Model

The volume fraction α is related to the distribution function through $\alpha = f(D)\frac{\pi D^3}{6}\Delta D$. By integrating Eq. (3) over the droplet diameter D (taking the limit $\Delta D \to dD$), it is possible to show that

$$\frac{\partial M^{(3)}}{\partial t} + \boldsymbol{\nabla}\cdot(M^{(3)}\mathbf{u}^{(3)}) = \Gamma_{M^{(3)}}, \tag{11}$$

which represents a transport equation for the 3^{rd} moment of the distribution. Note that the quantity $\mathbf{u}^{(3)}$ appeared as an outcome of the integration over the size spectrum. Using the same integration procedure for the momentum equation leads to:

$$\frac{\partial M^{(3)}\rho_d\mathbf{u}^{(3)}}{\partial t} + \boldsymbol{\nabla}\cdot\Big(\int_0^\infty fD^3\,\rho_d\mathbf{u}\,\mathbf{u}\,dD\Big) = \int_0^\infty \mathbf{M}dD + \boldsymbol{\nabla}\cdot\Big(\int_0^\infty fD^3\,\boldsymbol{\tau_d^t}\,dD\Big) + \Gamma_{M^{(3)}}\,\mathbf{u}^{(3)}. \tag{12}$$

The integrals in the above equation will be dealt with on a term by term basis. To recast the second term on the LHS, following the decomposition proposed by Beck and Watkins (2003), the particle velocities $\mathbf{u}$ are written in terms of the volume average velocity $\mathbf{u}^{(3)}$ plus a relative velocity component (representing the deviation from the average) $\mathbf{u}'$: $\mathbf{u} = \mathbf{u}^{(3)} + \mathbf{u}'$. As a first approximation, the term involving the velocity deviation tensor having order of magnitude $O(\mathbf{u}'\mathbf{u}')$ will be neglected. This will certainly be a good approximation if the major contribution to the total momentum of the particles comes from the bigger size classes, and these do not deviate much from $\mathbf{u}^{(3)}$. However, the assessment of its importance – which requires closure for the velocity distribution $\mathbf{u}(D)$ – will be left for future investigation.

On the RHS, the integral of the momentum exchange term $\mathbf{M}$ leads, for the pressure and shear stress contribution, to:

$$\int_0^\infty fD^3\,\boldsymbol{\nabla}p\,dD + \int_0^\infty fD^3\,\boldsymbol{\nabla}\cdot\boldsymbol{\tau_c}\,dD = M^{(3)}\boldsymbol{\nabla}p + M^{(3)}\boldsymbol{\nabla}\cdot\boldsymbol{\tau_c}. \tag{13}$$

In order to integrate the drag and turbulent dispersion terms, the droplet relative velocity will be approximated by $\mathbf{u}_r = \mathbf{u}^{(3)} - \mathbf{u}_c$. With this assumption, integration of Eq. (7) and Eq. (9) leads to:

$$\int_0^\infty \mathbf{M}_{Drag}dD = 18\mu_c\Big[M^{(1)} + 0.15\Big(\frac{|\mathbf{u}^{(3)} - \mathbf{u}_c|}{\nu_c}\Big)^{0.687}M^{(1.687)}\Big](\mathbf{u}^{(3)} - \mathbf{u}_c), \tag{14}$$

and

$$\int_0^\infty \mathbf{M}_{TD}dD = 18\mu_c\frac{\nu_c^t}{\sigma_\alpha}\Big[\boldsymbol{\nabla}M^{(1)} + 0.15\Big(\frac{|\mathbf{u}^{(3)} - \mathbf{u}_c|}{\nu_c}\Big)^{0.687}\boldsymbol{\nabla}M^{(1.687)}\Big]. \tag{15}$$

The turbulent stress term is approximately evaluated using the volume average velocity $\mathbf{u}^{(3)}$ and the third moment $M^{(3)}$.

The integration of the energy equation – with a similar treatment for the convective term as used in the momentum equation – leads to the conservation equation of the volume average internal energy:

$$\frac{\partial M^{(3)}\rho_d i^{(3)}}{\partial t} + \boldsymbol{\nabla}\cdot(M^{(3)}\rho_d \mathbf{u}^{(3)} i^{(3)} - M^{(3)}\frac{\nu_d^t}{\mathrm{Pr}_t^d}\boldsymbol{\nabla}T^{(3)}) \quad = \quad \Gamma_{M^{(3)}}\hat{h}^{(3)} + Q, \tag{16}$$

with $\hat{h}^{(3)}$ determined by: $\hat{h}^{(3)} = i^{(3)} + \Delta h_v$. The integral heat flux Q is finally given by:

$$Q \quad = \quad \pi\lambda_c\Big[2M^{(1)} + 0.6\Big(\frac{|\mathbf{u}^{(3)} - \mathbf{u}_c|}{\nu_c}\Big)^{\frac{1}{2}} M^{(1.5)}\mathrm{Pr}^{\frac{1}{3}}\Big](T^{(3)} - T_c). \tag{17}$$

Here, the droplet temperature at a given position is considered independent of the diameter. This hypothesis will be shown to suffice for the present purposes, but the more general case requires the consideration of other average quantities (for example, a surface average temperature to be used with the evaporation models) and will be analyzed in future work.

2.2.1 Moments Transport Equations

The moments transport equations can be written in a generalized form as:

$$\frac{\partial M^{(k)}}{\partial t} + \boldsymbol{\nabla}\cdot(\mathbf{u}^{(k)}M^{(k)}) \quad = \quad \Gamma_{M^{(k)}}, \tag{18}$$

with $\Gamma_{M^{(k)}}$ the source terms resulting from evaporation. The advection of moments by the continuous phase is an important aspect of the model which was explored in detail by Carneiro, Kaufmann and Polifke (2008). However, for the description of the spray used herein, the moment transport velocities will be considered equal to the volume average velocity, $\mathbf{u}^{(3)}$. Polydispersity is achieved by considering different source terms due to evaporation for each moment transport equation. The development of these source terms is demonstrated next.

2.3 Droplet Evaporation

The overall effect of evaporation on size distribution is that of decreasing all moments $M^{(k)}$'s, once they represent integral characteristics of the whole spectrum of droplet sizes (total volume, surface, etc). The source terms $\Gamma_{M^{(k)}}$ can be developed from physical principles governing the evaporation process, as suggested by Beck and Watkins (2003). For the diffusion controlled, quasi-steady evaporation of single component spherical droplets of a certain size class, the total rate of evaporation (per unit volume) is given by:

$$\Gamma_d \quad = \quad -6\frac{\alpha}{D^2}\rho_c\,\mathfrak{D}\,\mathrm{Sh}\,ln(1+B_M), \tag{19}$$

with the Sherwood number (Sh) given by: $\mathrm{Sh} = 2 + 0.6\mathrm{Re}^{\frac{1}{2}}\mathrm{Sc}^{\frac{1}{3}}$. The evaporative Nusselt number is corrected through the expression $\mathrm{Nu}^* = \mathrm{Nu}\frac{ln(1+B_M)}{B_M}$. The Spalding number B_M is in turn given by

$$B_M \quad = \quad \frac{Y_s - Y_v}{1 - Y_s}, \tag{20}$$

with Y_v the fuel vapor mass fraction. Its value at the droplet surface (Y_s) is given by

$$Ys \quad = \quad \Big[1 + \frac{W_G}{W_F}\Big(\frac{p}{p_v} - 1\Big)\Big]^{-1}, \tag{21}$$

where W_G and W_F are the molecular weights of gas and fuel, respectively. The vapor pressure is determined by the Clausius-Clapeyron relation

$$p_v \quad = \quad p_{\mathrm{ref}}\exp\Big[-\frac{\Delta h_v}{R}\Big(\frac{1}{T^{(3)}} - \frac{1}{T_{\mathrm{ref}}}\Big)\Big], \tag{22}$$

where p_{ref} and T_{ref} are reference pressure and temperature, respectively. To determine the diffusion coefficient $\mathfrak{D}$, a Lewis number of unity is assumed, with $\rho_c\mathfrak{D} = \frac{k_c}{c_{p,c}}$. k_c and $c_{p,c}$ are thermal conductiviy and specific heat of the

continuous phase, respectively. Thus, integrating Eq. (19) over the whole spectrum allows to compute the source term $\Gamma_{M^{(3)}}$:

$$\Gamma_{M^{(3)}} = -\frac{6}{\rho_d}\frac{k_c}{c_{p,c}}\, ln(1+B_M)\Big[2M^{(1)} + 0.6\Big(\frac{|\mathbf{u}^{(3)}-\mathbf{u}_c|}{\nu_c}\Big)^{\frac{1}{2}} M^{(1.5)}\mathrm{Sc}^{\frac{1}{3}}\Big]. \tag{23}$$

Similarly, $\Gamma_{M^{(2)}}$ and $\Gamma_{M^{(1)}}$ can be computed from:

$$\Gamma_{M^{(2)}} = -\frac{4}{\rho_d}\frac{k_c}{c_{p,c}}\, ln(1+B_M)\Big[2M^{(0)} + 0.6\Big(\frac{|\mathbf{u}^{(3)}-\mathbf{u}_c|}{\nu_c}\Big)^{\frac{1}{2}} M^{(0.5)}\mathrm{Sc}^{\frac{1}{3}}\Big] \tag{24}$$

and

$$\Gamma_{M^{(1)}} = -\frac{2}{\rho_d}\frac{k_c}{c_{p,c}}\, ln(1+B_M)\Big[2M^{(-1)} + 0.6\Big(\frac{|\mathbf{u}^{(3)}-\mathbf{u}_c|}{\nu_c}\Big)^{\frac{1}{2}} M^{(-1.5)}\mathrm{Sc}^{\frac{1}{3}}\Big]. \tag{25}$$

2.3.1 Closure through a pNDF

Due to the form of mass, momentum and heat exchange expressions used, the integration of droplet equations causes the appearance of unknown moments ($M^{(1.687)}$, $M^{(1.5)}$, etc) in the formulation. These quantities are a priori unknown, giving rise to a closure problem. A simple way to overcome this issue is to assume the functional form of $f(D)$ (a presumed Number Density Function – pNDF), calculating unknown moments after reconstruction of the distribution using lower order ones. Here, the Gamma distribution function is chosen, since it is able to represent a wide variety of size distribution spectra. Furthermore, its reconstruction from (any) 3 consecutive lower order moments is straightforward, making it very suitable for the present purposes (although other functional forms can be easily incorporated in the model). Hence, if $f(D)$ is given by a Gamma function:

$$f(D) = C_0 \frac{D^{q-1}e^{-\frac{D}{p}}}{p^q\Gamma(q)}, \tag{26}$$

moments can be explicitly calculated by the general expression:

$$M^{(k)} = C_0 \frac{\Gamma(q+k)p^k}{\Gamma(q)}, \tag{27}$$

with the parameters p, q and C_0 being given by

$$\begin{aligned} p &= \frac{M^{(k_{min}+2)}M^{(k_{min})} - (M^{(k_{min}+1)})^2}{M^{(k_{min})}M^{(k_{min}+1)}} \\ q &= \frac{(k_{min}+1)(M^{(k_{min}+1)})^2 - k_{min}M^{(k_{min}+2)}M^{(k_{min})}}{M^{(k_{min}+2)}M^{(k_{min})} - (M^{(k_{min}+1)})^2} \end{aligned} \tag{28}$$

$$C_0 = \begin{cases} \frac{M^{(k_{min})}}{\alpha^{k_{min}}\Pi_{l=0}^{k_{min}-1}(q+l)} & \text{if } k_{min} \in N^+ \\ M^{(0)} & \text{if } k_{min} = 0 \end{cases}$$

where $k_{min} = 1$ was chosen in order to ensure volume conservation by using $M^{(3)}$ in the reconstruction process. Hence, the complete model requires the solution of Eq. (18) for $M^{(1)}$-$M^{(3)}$.

2.3.2 Conditions for a Valid Moment Set

The most straightforward way to check the validity of a moment set is by calculating the convexity condition:

$$M^{(k)}\,M^{(k-2)} - (M^{(k-1)})^2 > 0. \tag{29}$$

For the Gamma distribution used in the present work, $k = 3$ corresponds to conditions necessary to avoid negative values of the NDF, which is clearly unphysical. This criterion is a necessary but not sufficient condition for a valid

moment set. Necessary and sufficient conditions for existence of a distribution function given a set of moments ($M^{(k)}$, $k = 0,\ 1,\ 2...2l + 1$) are non-negative Hankel-Hadamard determinants (see Shohat and Tamarkin, 1963):

$$\mathbf{\Delta_{k,l}} = \begin{pmatrix} M^{(k)} & M^{(k+1)} & \dots & M^{(k+l)} \\ M^{(k+1)} & M^{(k+2)} & \dots & M^{(k+l+1)} \\ \vdots & \vdots & \ddots & \vdots \\ M^{(k+l)} & M^{(k+l+1)} & \dots & M^{(k+2l)} \end{pmatrix} \geq 0$$

with $k = 0, 1$; $l \geq 0$; $\mathbf{\Delta_{k,l}} = 0$ for a monodisperse distribution.

The advection of moments and source terms due to evaporation might give rise to invalid sets during the simulation – even if boundary conditions are such leading to valid ones. The *ad hoc* correction of the moments is expected to be a necessary step specially if they are transported with different velocities. However, as will be shown later, this procedure was not necessary here, and the variation of the moments caused by evaporation led to physical distributions throughout the whole solution domain, with no need for bounding the Gamma parameters obtained in the reconstruction process.

2.4 Gas Phase Equations

For the gas phase, the mass conservation can be written as:

$$\frac{\partial \alpha_c \rho_c}{\partial t} + \boldsymbol{\nabla} \cdot (\alpha_c \rho_c \, \mathbf{u}_c) \quad = \quad -\Gamma \quad (= -\rho_d \frac{\pi \Gamma_{M^{(3)}}}{6}). \tag{30}$$

Furthermore, the constraint $\frac{\pi M^{(3)}}{6} + \alpha_c = 1$ must be satisfied. The momentum equation is:

$$\frac{\partial \alpha_c \rho_c \mathbf{u}_c}{\partial t} + \boldsymbol{\nabla} \cdot (\alpha_c \rho_c \, \mathbf{u}_c \mathbf{u}_c) \quad = \quad -\alpha_c \boldsymbol{\nabla} p + \boldsymbol{\nabla} \cdot (\alpha_c \boldsymbol{\tau_c}) - \int_0^\infty (\mathbf{M}_{Drag} + \mathbf{M}_{TD}) dD - \Gamma \, \mathbf{u}^{(3)}, \tag{31}$$

with the stress tensor given by $\tau_c = \mu_c^{eff}(\boldsymbol{\nabla}\mathbf{u}_c + \boldsymbol{\nabla}\mathbf{u}_c^T) - \frac{2}{3}(\mu_c^{eff}\boldsymbol{\nabla} \cdot \mathbf{u}_c + \rho_c k)\,\mathbf{I}$. The effective viscosity is calculated by the sum of molecular and turbulent viscosity: $\mu_c^{eff} = \mu_c + \mu_c^t$.

The internal energy equation is written as:

$$\frac{\partial \alpha_c \rho_c i_c}{\partial t} + \boldsymbol{\nabla} \cdot (\alpha_c \rho_c \, \mathbf{u}_c i_c - \alpha_c \rho_c \frac{\nu_c^{eff}}{\mathrm{Pr}_t^c} \boldsymbol{\nabla} T_c) \quad = \quad -p \, \boldsymbol{\nabla} \cdot \mathbf{U} - \Gamma \hat{h}^{(3)} - Q, \tag{32}$$

with $\mathbf{U} = \alpha_c \mathbf{u}_c + (1 - \alpha_c)\mathbf{u}^{(3)}$. The transport equation for the fuel vapor mass fraction Y_v needed by the evaporation model is given by:

$$\frac{\partial \alpha_c \rho_c Y_v}{\partial t} + \boldsymbol{\nabla} \cdot (\alpha_c \rho_c \, \mathbf{u}_c Y_v - \alpha_c \frac{\nu_c^{eff}}{\mathrm{Sc}_t^c} \boldsymbol{\nabla} Y_v) \quad = \quad -\Gamma. \tag{33}$$

For simplicity, and due to the small temperature and pressure variations expected, as well as small fuel vapor mass fraction, gas properties were considered constant during the simulation.

2.4.1 Turbulence Modeling

The turbulence model used herein is the two-phase $k-\epsilon$ model, as described by Oliveira and Issa (1998). The equations for the transport of turbulence kinetic energy k_c and its rate of dissipation ϵ_c, for the continuous phase, are written as:

$$\frac{\partial \alpha_c \rho_c k_c}{\partial t} + \boldsymbol{\nabla} \cdot (\alpha_c \rho_c \, \mathbf{u}_c k_c) \quad = \quad \boldsymbol{\nabla} \cdot (\alpha_c \frac{\mu_c^t}{\sigma_k} \boldsymbol{\nabla} k_c) + \alpha_c (G - \rho_c \epsilon_c) + S_d^k - \Gamma k_c \tag{34}$$

and

$$\frac{\partial \alpha_c \rho_c \epsilon_c}{\partial t} + \boldsymbol{\nabla} \cdot (\alpha_c \rho_c \, \mathbf{u}_c \epsilon_c) \quad = \quad \boldsymbol{\nabla} \cdot (\alpha_c \frac{\mu_c^t}{\sigma_\epsilon} \boldsymbol{\nabla} \epsilon_c) + \alpha_c \frac{\epsilon_c}{k_c} (C_1 G - C_2 \rho_c \epsilon_c) + S_d^\epsilon - \Gamma \epsilon_c. \tag{35}$$

In the above equations, the turbulent viscosity μ_c^t and the generation of k_c are computed from:

$$\mu_c^t = \rho_c C_\mu \frac{k_c^2}{\epsilon_c} \tag{36}$$

and

$$G = \mu_c^t \boldsymbol{\nabla}\mathbf{u}_c \cdot (\boldsymbol{\nabla}\mathbf{u}_c + \boldsymbol{\nabla}\mathbf{u}_c^T). \tag{37}$$

Γk_c and $\Gamma \epsilon_c$ are the additional source terms due to droplet evaporation. In addition, S_d^k and S_d^ϵ represent the interaction between the disperse phase and continuous phase turbulence, which are given by:

$$S_d^k = -K_a\Big[2\alpha_d\alpha_c(1-C_k)\,k_c + \frac{\nu_c^t}{\sigma_\alpha}\boldsymbol{\nabla}\alpha_d \cdot (\mathbf{u}^{(3)} - \mathbf{u}_c)\Big] \tag{38}$$

$$S_d^\epsilon = -2\alpha_d\alpha_c(1-C_k)\,\epsilon_c\,K_a. \tag{39}$$

In the above equations, K_a and C_k are given by:

$$K_a = 18\mu_c\Big[M^{(1)} + 0.15\Big(\frac{|\mathbf{u}^{(3)} - \mathbf{u}_c|}{\nu_c}\Big)^{0.687} M^{(1.687)}\Big] \tag{40}$$

and

$$C_k = \sqrt{C_t}, \tag{41}$$

respectively. The model for the response coefficient C_t employed here was the same used by Oliveira and Issa (1998). It is given by:

$$C_t = \frac{3+\beta}{1+\beta+2\frac{\rho_d}{\rho_c}}, \tag{42}$$

with

$$\beta = \frac{\tau_{\epsilon_c}}{\tau_p}\Big(1+2\frac{\rho_d}{\rho_c}\Big). \tag{43}$$

τ_{ϵ_c} and τ_p are the turbulence time scale and particle relaxation time, respectively, which are given by the expressions $\tau_{\epsilon_c} = 0.41\frac{k_c}{\epsilon_c}$ and $\tau_p = \frac{\rho_d}{K_a}$.

The turbulent kinetic energy (k_d) and turbulent viscosity (ν_d^t) of the disperse phase are simply given by the relations: $k_d = C_k k_c$ and $\nu_d^t = C_k \nu_c^t$. Finally, the $k-\epsilon$ constants used herein were that of the standard model (see, e.g., Rusche, 2002), with the turbulent quantities Pr^t and Sc^t taken to be unity for both phases.

3. NUMERICAL MODEL

OpenFOAM is a C++ class library which can be used to develop CFD codes for a wide variety of problems, including multiphase flows, with many capabilities of the finite volume method available (see Weller et al. 1998). The implementation of additional transport equations for the moments and sub-models for the mass, momentum and heat exchange terms, as well as the energy equation, is done within a steady state version of the `twoPhaseEulerFoam` solver with an adapted SIMPLE algorithm. A full description of the Two-Fluid Model implemented in OpenFOAM can be found in the work of Rusche (2002), and the implementation of the moments transport equations was illustrated by Carneiro, Kaufmann and Polifke (2008). In the present work, the energy equations are incorporated in the pressure-velocity system, and the pressure equation was modified to account for mass exchange between phases. Source terms due to evaporation and heat exchange were handled implicitly whenever possible, otherwise all numerical schemes were chosen in line with Rusche (2002) and Carneiro, Kaufmann and Polifke (2008).

4. TEST CASE

Figure (1) sketches the geometry of the test case. An axisymmetric domain is used to represent the experimental set-up of Baessler, Moesl and Sattelmayer (2007). The atomizer is placed centrally to a tube with 71 mm diameter and 610 mm length. Fuel is fed to an ultrasonic nozzle at 15 ml/min, which uses a small mass flow of carrier air to improve droplet dispersion. Main air flow is injected at a substantially higher flow rate (285 ln/min) than the atomizing air (15 ln/min), flowing through an annular passage 71 mm long, mixing with secondary air flow and spray. Main air temperature was 90 C for the evaporating case, otherwise all fluids were at 25 C. The outlet section was prescribed at 1 atm and all walls were considered adiabatic. Boundary conditions for the moments were calculated from the experimentally determined distribution measured at 8 mm behind the oscillating plate where droplets were generated: $M^{(1)} = 3.83 \cdot 10^5$ m^{-2}, $M^{(2)} = 1.43 \cdot 10^1$ m^{-1} and $M^{(3)} = 6.36 \cdot 10^{-4}$.

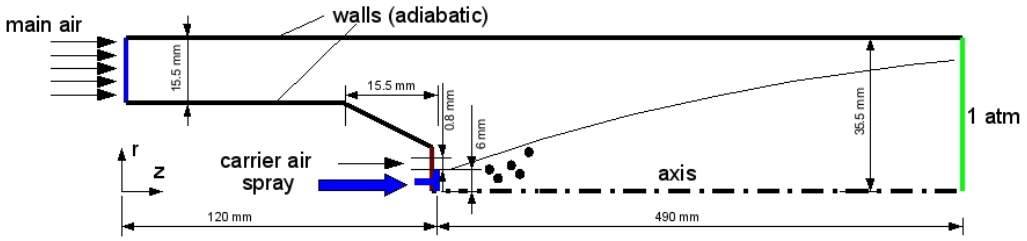

Figure 1. Sketch of the geometry used in the test case.

4.1 Non-Evaporating Case

Comparison of the axial and radial velocity profiles at two positions along the z-coordinate (8 mm and 150 mm behind the oscillating plate) is shown in Fig. (2). The two distinct streams observed near the spray inlet tend to mix towards the outlet of the pipe, where a more uniform axial velocity profile is observed and the radial component becomes marginal. A good quantitative agreement can be observed between both components of the disperse phase volume average velocity $\mathbf{u}^{(3)}$ and mean droplet velocity from PDA measurements of Baessler, Moesl and Sattelmayer (2007). At the first axial position, the location and width of velocity peaks for both components is well captured by the model, even though its values seem to be slightly underpredicted, not following the continuous phase velocity as readily as the data suggests. This might be an artifact produced by the type of average used to compute mean velocities from experiments; a number average, *not* a volume one. Another possible reason for the deviation is the assumption of constant velocity used for the integration of drag and turbulent dispersion forces, which might fail specially in regions where a high acceleration occurs. At the second axial position further downstream in the pipe, continuous phase and disperse phase velocities are nearly equal and agree well with the experimental profile.

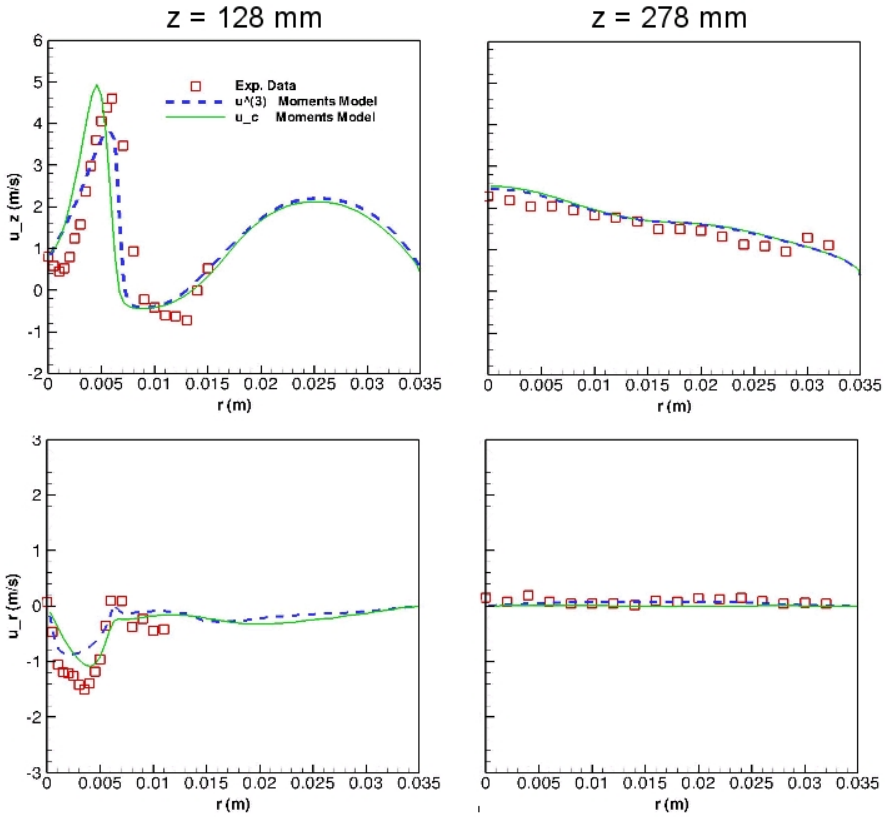

Figure 2. Axial (top) and radial (bottom) velocity profiles at two positions along the tube – z = 128 mm (left) and z = 278 mm (right).

4.2 Evaporating Case

Contours of the disperse phase volume fraction ($\propto M^{(3)}$) and vapor mass fraction (Y_v) are shown in Fig. (3). A higher concentration of droplets is observed near the inlet, which gradually decreases towards the end of the pipe due to both dispersion and evaporation of the droplets, while the amount of vaporized fuel increases. The low order Hankel-Hadamard determinants Δ_{02} and Δ_{11} containing the most relevant moments were assessed in order to check the signature of invalid moment sets throughout the solution domain. Also depicted in Fig. (3), both determinants are positive within the spray and tend to zero towards the outside region (small $M^{(3)}$). Reconstructed distributions at the centerline show the effect of evaporation as the droplets travel downstream in the pipe, diminishing the total population in the spray. Disperse phase

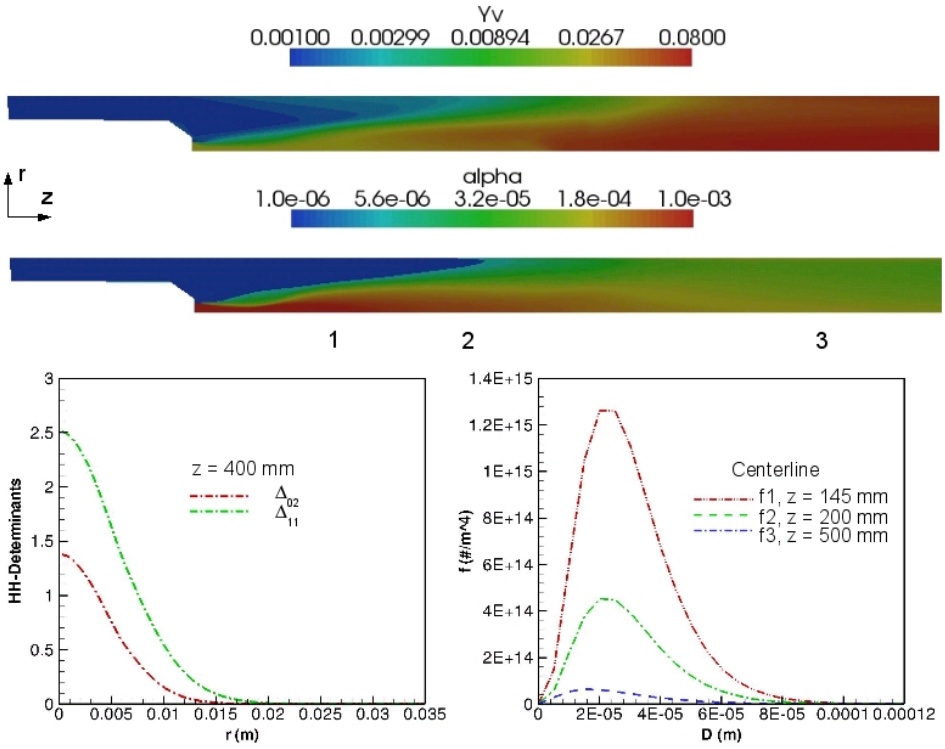

Figure 3. Contours of the disperse phase volume fraction (top); Hankel-Hadamard determinants for axial coordinate z = 400 mm (bottom-left) and reconstructed distributions at the centerline for positions 1 (z = 145 mm), 2 (z = 200 mm) and 3 (z = 500 mm).

mass flux for three axial positions (z = 200, 400 and 600 mm) and droplet mean diameters profiles corresponding to z = 600 mm are shown in Fig. (4). The mean diameters are defined as the ratio between moments of the size distribution function and can be written in a generalized form as $D_{mn} = \left(\frac{M^{(m)}}{M^{(n)}}\right)^{\left(\frac{1}{m-n}\right)}$. The mass flux is in turn defined as: $\dot{m}'' = \rho_d \frac{\pi}{6} D_{30}^3 u_z^{(3)} M^{(0)}$; $u_z^{(3)}$ is the axial component of $\mathbf{u}^{(3)}$. The evolution of mass flux profiles clearly shows the effect of spray evaporation while the droplet-hot air mixture travel towards the pipe outlet. The profile at z = 600 mm compares well with the data, indicating that the degree of vaporization could also be reproduced by the model. Furthermore, as shown by the experimental measurements, the mean diameters are approximately constant at z = 600 mm in most part of the spray and tend to slightly diminish in the main hot air stream, mainly because the temperature is higher there (but probably also because bigger droplets tend to travel near the centerline). This effect was also captured by the Moments Model through the implementation of source terms described earlier but an increase is also observed in the trends of the curves. This occurs due to the nature of the source terms for the moments, which reproduces the D^2-Law: smaller droplets have higher rate of evaporation, which translates into higher rates of evaporation for low order moments. Towards the spray tip and near the wall, only a few smaller droplets are likely to be found leading to a decrease in the mean diameters.

5. CONCLUSION

A new Moments Model for polydisperse spray flows was developed and implemented within the open source code OpenFOAM. The model derivation was achieved through integration of the droplet equations over the size spectrum, yielding a formulation depending on the moments and their respective transport velocities. Due to the form of mass, mo-

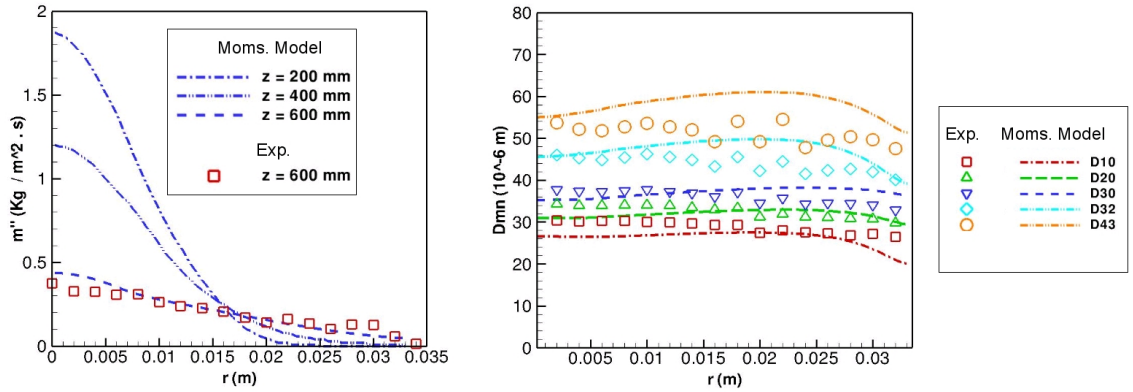

Figure 4. Comparison of mass fluxes (z = 200, 400 and 600 mm) and droplet mean diameters (z = 600 mm) obtained with the Moments Model and PDA data.

mentum and heat exchange terms, unclosed quantities appear in the sub-models, which were handled through a presumed distribution function of Gamma type. The model was applied in a configuration comprising of a spray generated by an ultra-sonic atomizer in both non-evaporative and evaporative cases. A good agreement was observed indicating that the Moments Model is able to correctly describe the radial dispersion of the droplets during the mixing process of the two air streams throughout the pipe. For the evaporative case, experimentally determined mean diameters and disperse phase mass flux could be well reproduced by the model through the implementation of moments source terms derived from the D^2-Law. Hankel-Hadamard determinants were observed to be always positive, confirming the validity of the moments sets, which were able to reproduce physical distributions throughout the whole flow field. Future work involves the development and incorporation of multi-velocity and multi-temperature effects into the existing model, and its validation against pratical applications.

6. ACKNOWLEDGEMENTS

The authors want to acknowledge the financial support given by CNPq (Brazilian National Council for Research and Technological Development) and GRS (Gesellschaft für Reaktorsicherheit).

7. REFERENCES

Baessler, S., Moesl, K., Sattelmayer, T., 2007, "NOx emissions of a premixed partially vaporized kerosene spray flame", Journal of Engineering for Gas Turbines and Power, Vol. 129, pages 695-702.

Beck, J. C., Watkins, A. P., 2003, "On the Development of a Spray Model Based on Drop-Size Moments", Proc. R. Soc. Lond. A., Vol. 459, pp. 1365-1394.

Carneiro, J. N. E., Kaufmann, V., Polifke, W., 2008, "Implementation of a moments model in OpenFOAM for polydispersed multiphase flows"; Open Source CFD International Conference 2008, Berlin, Germany.

Fox, R. O., Laurent, F., Massot, M., 2008, "Numerical simulation of spray coalescence in an Eulerian framework: Direct quadrature method of moments and multi-fluid method", J. Comp. Physics, Vol. 227, pp. 3058-3088.

Oliveira, J. P., Issa, R. I., 1998, "Numerical prediction of particle dispersion in a mixing layer using an eulerian two-phase flow model", Proceedings of FEDSM98 ASME Fluids Engineering Division Summer Meeting, Washington, DC.

Mostafa, A. A., Mongia, H. C., 1987, "On the Modelling of Turbulent Evaporating Sprays: Eulerian versus Lagrangian Approach", Int. J. of Heat and Mass Transfer, Vol. 30, pp. 2583-2593.

Rusche, H., 2002, "Computational Fluid Dynamics of Dispersed Two-Phase Flows at High Phase Fractions", PhD Thesis, Imperial College of Science Technology and Medicine, London, UK.

Shohat, J. A., Tamarkin, J. D., 1963, "The Problem of Moments", Providence, RI: American Mathematical Society.

Crowe, C. T., Sommerfeld, M., Tsuji, Y., 1998, "Multiphase flows with droplets and particles", CRC Press, NY.

Weller, H. G., Tabor, G., Jasak, H., Fureby, C., 1998, "A tensorial approach to computational continuum mechanics using object-oriented techniques", Computers in Physics, Vol. 12, Nr. 6, pp. 620-631.

Wright Jr., D. L., 2007, "Numerical Advection of Moments of the Particle Size Distribution in Eulerian Models", Journal of Aerosol Science, Vol. 38, pp. 352-369.

8. Responsibility notice

The authors are the only responsible for the printed material included in this paper